MHC class I complexes loaded by a periodate trigger

Boris Rodenko,[1] Mireille Toebes,[2] Patrick H.N. Celie,[3] Anastassis Perrakis,[3]

Ton N. M. Schumacher[2] & Huib Ovaa[1]

[1] Division of Cell Biology II

[2] Division of Immunology

[3] Division of Biochemistry

The Netherlands Cancer Institute, Plesmanlaan 121, 1066 CX, Amsterdam, The Netherlands.

Author contributions:

BR, MT and PC performed experiments

BR, PC, AP, TS and HO designed experiments

BR, PC, AP, TS and HO wrote the manuscript

Correspondence should be addressed to T.N.M.S. (t.schumacher@nki.nl) or H.O. (h.ovaa@nki.nl)

Abstract

Class I major histocompatibility complexes (MHC) present peptide ligands on the cell surface for recognition by appropriate cytotoxic T cells. The unstable nature of unliganded MHC necessitates the production of recombinant class I complexes through *in vitro* refolding reactions in the presence of an added excess of peptides. This strategy is not amenable to high-throughput production of vast collections of class I complexes. To address this issue, we recently designed photocaged MHC ligands that can be cleaved by a UV light trigger in the MHC bound state under conditions that do not affect the integrity of the MHC structure.

The results obtained with photocaged MHC ligands demonstrate that conditional MHC ligands can form a generally applicable concept for the creation of defined peptide-MHC complexes. However, the use of UV exposure to mediate ligand exchange is unsuited for a number of applications, due to the lack of UV penetration through cell culture systems and due to the transfer of heat upon UV irradiation which can induce evaporation. To overcome these limitations, here, we provide proof-of-concept for the generation of defined peptide-MHC complexes by chemical trigger-induced ligand exchange. The crystal structure of the MHC complex with the novel chemosensitive ligand, showcases that the ligand occupied the expected site binding site, in a conformation where the hydroxyl groups should be reactive to periodate. We proceed to validate this technology by producing peptide-MHC complexes that can be used for T cell detection. The methodology that we describe here should allow loading of MHC complexes with defined peptides in cell culture devices, thereby permitting antigen-specific T cell expansion and purification for cell therapy. In addition, this technology will be useful to develop miniaturized assay systems for performing high-throughput screens for natural and unnatural MHC ligands.

Introduction

The concept of caged MHC class I ligands. The heterotrimeric major histocompatibility class I complexes (MHC class I) comprise an invariant light chain called β2-microglobulin, a polymorphic heavy chain and a peptide ligand normally 8 to 11 amino acids in length. Surveillance of the surface composed by both the peptide ligand and part of the heavy chain by T cell receptors on cytotoxic T cells forms the basis for a subsequent antigen-specific cytotoxic T cell response. Association of peptides with MHC class I is largely based on complementarity of amino acid side-chains at defined anchor positions in the MHC structure[1,2] and by ionic interactions of their charged peptide acid and base termini[3,4].

The assembly of MHC class I complexes critically depends on availability of peptides that are essential for the stability of the MHC class I complex[5,6], as evidenced by the effects of depletion of this peptide supply. This unstable nature of unliganded MHC demands the production of recombinant MHC through *in vitro* refolding reactions in the presence of an added excess of peptides[7]. However, the elaborate nature of these methods hampers their utility for parallel production of collections of peptide-MHC (pMHC) complexes and, as a consequence, our current understanding of T cell recognition is limited to only a small fraction of the available pMHC repertoire. To address this issue we have set out to develop MHC ligands that can be made to dissociate from the MHC complex by application of a defined trigger, thereby allowing parallel loading with ligands of interest. As a first generation of such conditional MHC ligands we have designed photocaged MHC ligands that can be cleaved by a UV trigger in the MHC bound state under conditions that do not affect the integrity of the MHC structure (Fig. 1a and b) (Celie et al, manuscript submitted)[8-10]. MHC class I complexes occupied with such photocaged ligands can be produced and purified using standard strategies. Cleaved fragments produced upon photolysis are no longer docked through double anchor residues and lose most of the original affinity resulting in dissociation from the MHC, leaving an unstable, peptide-receptive complex that gradually denatures (Fig. 1a). Importantly, photolysis in the presence of another peptide ligand results in net ligand exchange, leading to a class I complex charged with an epitope of choice. Following the first description of this general approach in 2006, ligands that disintegrate upon application of a photostimulus have been developed for 9 different MHC products,

i.e. human MHC class I HLA-A1, -A2, -A3, -A11 and -B7,[8-10] murine MHC class I H2-D^b, H2-K^b [8,11,12] and H2-L^d [13], and human MHC class II HLA DR2[14].

Caged MHC class ligands and their use. Conditional exchange strategies enable the generation of peptide-receptive MHC complexes under physiological conditions and these MHC molecules have been used to identify peptide epitopes from disease-specific antigens that bind to the MHC allele under investigation. Furthermore, peptide-MHC complexes produced by MHC exchange reactions can be used to prepare collections of MHC tetramers (or other multimeric MHC reagents) for the detection of antigen-specific T cells by flow cytometry. Using such exchange tetramers we have validated the feasibility of large scale screening approaches by the definition of cytotoxic T cell epitopes within the H5N1 influenza A/Vietnam/1194/04 genome[8]. In subsequent work, this technology has proven useful for the identification of human and murine T cell epitopes in Chlamydia,[11] murine gamma herpes virus,[12] Toxoplasma gondii[13] and melanoma-associated antigens (ref [10] and Reker-Hadrup et al. manuscript submitted).

Conditional ligands and photo- vs chemocleavage. Although current phototriggered exchange methodology has proven very suitable for the parallel generation of MHC reagents, it is not optimal for all applications that can be envisaged for this technique. First, to reduce the risk of false positives (or negatives) resulting from high-throughput screening campaigns, uniform cleavage conditions need to be ascertained, while uniform parallel UV irradiation might be difficult to achieve when screening large numbers of potential ligands in minute volumes. Second, the deposition of pMHC complexes on solid surfaces to probe T cell function has been proven possible[15-17], and the resulting pMHC microarrays may in principle be generated by *in situ* exchange reactions. However, the heat generated by UV irradiation of surfaces commonly in use in microarray technologies and resulting evaporation prohibits the use of a UV method for this particular application. Third, the *in situ* coating of conditional MHC complexes with peptide antigens by ligand exchange would form an attractive strategy for the generation of pMHC-coated culture devices that can be used for T cell expansion and enrichment. However, UV-irradiation is less suited for such tissue culture applications as common culture plastics hamper efficient transmission of UV light required for photo-uncaging.

For these reasons, we investigated the option of using a chemical trigger to effect peptide exchange reactions. Advantages are several-fold: exchange rates can simply be controlled by dosing the amount of chemical trigger reagent, while the trigger is compatible with sterile conditions where necessary and compatible with plastics, requirements not easily unified in a combination of UV irradiation and standard tissue culture practice. Importantly, a chemical trigger is readily available, allows the option of quenching of the triggering reagent and obviates the need for any special equipment, thereby opening MHC ligand exchange technology to the wider scientific community.

Results

Conditional ligand screening. We took advantage in our design of the reactivity of the vicinal diol moiety, that is cleaved by the mild oxidant $NaIO_4$ under formation of two aldehyde species (Fig 1c), as periodate has proven compatible with (non-glycosylated) protein functionalities. As a building block for automated peptide synthesis we synthesized the isopropylidene protected diol (*2R,3R*)-4-*N*-Fmoc-amino-2,3-dihydroxybutanoic acid **IV** which is easily prepared on a large scale by the method of Kamiya et al.[18] starting from commercially available (−)-2,3-*O*-isopropylidene-D-erythronolactone **I** (Scheme 1).

For efficient chemocleavage of the conditional peptide to occur, accessibility of the diol containing amino acid residue to periodate anions is required and the vicinal hydroxyl groups must be oriented in such a fashion that formation of the cyclic periodate ester intermediate is allowed sterically. Crystal structures of HLA-A2.1 charged with viral epitopes show that 73 to 83% of the peptide is deeply buried into the MHC peptide binding groove.[19] A proven strategy for producing conditional MHC ligands is the replacement of one of the T cell receptor exposed amino acids in a known or predicted MHC ligand by an amino acid residue that is sensitive to a main chain breaking stimulus. In order to find a diol containing peptide that binds well to the MHC binding groove and that is, in turn, efficiently cleaved under mild oxidative conditions that do not compromise the integrity of the MHC protein, we scanned the diol containing γ-amino acid through the sequence of a number of known HLA-A2.1 nonameric and decameric epitopes between anchor positions p2 and p9 (for nonamers) or p10 (for decamers). As it seemed possible that periodate could diffuse into the peptide-binding groove, this unbiased approach for screening was chosen, rather than limiting such screening to known

exposed sites. Since the diol containing amino acid building block is a γ-amino acid, we hypothesized that two α-amino acid residues could be replaced by a single diol containing γ-amino acid, providing the rationale for our subsequent design. Accordingly, for the decameric epitopes we also synthesized their nonameric diol containing analogs. Parent peptides were included in the screen as controls. Peptides were generated by automated solid phase peptide synthesis and their purity was verified by LC/MS and found to be at least 85% for all peptides tested.

As conditional ligand cleavage by photolysis is orthogonal to chemically induced ligand cleavage, we evaluated the generated set of diol-containing peptides for MHC binding capacity by phototriggered peptide exchange methodology in 96 well format using biotinylated HLA-A2.1 charged with conditional peptide GILGFVFJ_1V, where J_1 is the photocleavable residue 3-amino 3-(2-nitro)phenyl propionic acid (see Table 1). Binding of the diol containing peptides to UV-vacated MHC complexes and susceptibility of the newly formed complex to $NaIO_4$ mediated cleavage were both assessed with a streptavidin-based ELISA assay[9]. In addition, MHC complexes loaded with diol containing peptides that showed efficient cleavage by $NaIO_4$ were subsequently tested for their capacity to allow chemically triggered peptide exchange. High photo-exchange efficiency combined with high $NaIO_4$ susceptibility were obtained with peptides **3**, **17**, **24** and **44**, all of them having the diol containing amino acid residue located on the p4 position. From this set, we selected peptide **3**, NVLBMVATV, where B is the diol containing amino acid residue, as conditional chemosensitive peptide of choice, because it gave the highest level of MHC recovery after chemically triggered peptide exchange (see Supporting Fig. 1).

Crystal structure of chemosensitive p*MHC complexes. A crystal structure of peptide **3**, lodged in the MHC peptide binding groove was obtained by UV mediated *in crystallo* exchange methodology (Celie et al, manuscript submitted) to obtain the complex with the NLVBMVATV peptide within the MHC crystals. The efficiency of peptide exchange was validated and confirmed efficient replacement of the photocleavable peptide for peptide NLVBMVATV. The diol containing peptide introduced by *in crystallo* exchange is located within the MHC peptide binding groove between the two α-helices from the α1 and α2 domains of the MHC heavy chain (Fig. 2a) and is in a clear conformation (Fig. 2b). The 2mFo-DF electron density map clearly shows the presence of peptide NLVBMVATV within the structure (Fig. 2b). We compared the structure of the peptide with its non-cleavable parent,

NLVPMVATV by superimposing the HLA-A2.1(Se-Mβ2m)::NLVBMVATV structure onto the previously solved HLA-A2.1::NLVPMVATV structure (Celie et al., manuscript submitted) (Fig. 2c). The peptides show a nearly identical structure, except for p4 and p5, where the diol containing peptide clearly adopts a different conformation. The diol residue was found to significantly protrude from the MHC peptide binding groove, making it accessible to the oxidizing reagent (Fig. 2a). Surface exposure of the p4 residue of the peptide is also observed in the parent structure and in other reported crystal structures of HLA-A2.1 loaded with various viral epitopes[19]. The dihedral angle between the vicinal hydroxyl groups however, seems to be limited to 70 degrees, which is apparently sufficient for reaction with the periodate anion[20]. Information on periodate reactivity towards 1,2-diols is limited towards open chain (*syn/anti*) and conformationally locked diols (*cis/trans*), where *trans* diols are generally uncleavable. It is of note that the dihedral angle in our conformationally locked diol is considerably greater than that of common *cis* diols, although some conformational freedom within the crystal may well be allowed. However, the orientation of both hydroxyl groups in the structure suggests that there may be opportunities to enhance the cleavage rate by enforcing a *cis*-conformation of these reactive hydroxyl groups during chemical synthesis.

Peptide cleavage and exchange kinetics. An LC/MS analysis of peptide **3** showed that upon treatment with $NaIO_4$ the peptide is fully cleaved into the two anticipated fragments (Supporting Fig. 3). In a kinetic experiment using HLA-A2.1 charged with fluorescently labeled NLVBMC(Fl)ATV peptide (Fl = tetramethylrhodamine-5-maleimide), exchange with native NLVPMVATV triggered by the addition of 0.3 mM $NaIO_4$ at rt was monitored by gel filtration HPLC (Fig. 3a). The higher retention time of MHC loaded with NLVBMC(Fl)ATV compared with MHC charged with NLVPMVATV is a consequence of the apolar character of the first. Fig. 3a shows that 2 h incubation is sufficient for >98% loss of the conditional ligand. In a control experiment, treatment of photolabile HLA-A2.1::KILGC(Fl)VFJ_1L under the same conditions (0.3 mM $NaIO_4$ and 50 μM NLVPMVATV) did not result in peptide exchange, not even after 16 h exposure to $NaIO_4$ (Fig. 3c). The release of fluorescently labeled remnants from the MHC binding groove revealed first order reaction kinetics (Supporting Fig. 4) with a $t_{1/2}$ of 0.51 h for the chemically triggered reaction, while for UV mediated cleavage a $t_{1/2}$ of 0.11 h was observed. Notably, while chemo-exchange reactions led to a reduction of fluorescence signal of >98%, we

consistently found that photomediated exchange reactions do not progress beyond 92% reduction in fluorescence signal, which has also been noted and discussed elsewhere[10].

Generation of MHC multimers for T cell detection by chemo-exchange. We used refolded and biotinylated HLA-A2.1::NLVBMVATV for MHC exchange reactions and converted these MHC exchange reagents into tetramers by addition of phycoerythrin (PE) conjugated streptavidin. The resulting reagents were used to detect antigen-specific T cells in peripheral blood samples by flow cytometry. Chemo-exchange tetramers containing the influenza A $M1_{(58-66)}$ epitope GILGFVFTL stain a low-frequency $M1_{(58-66)}$–specific T cells in peripheral blood from a healthy individual at least as efficiently as photo-exchange MHC class I tetramers (Fig. 4).

Whereas photo-exchange tetramers containing the CMV $pp65_{(495-503)}$ epitope NLVPMVATV stain low-magnitude peripheral blood mononuclear cells (PBMCs) from an HLA-A2.1 positive individual, the corresponding chemo-exchange tetramers give lower staining efficiency. LC/MS analysis revealed that under the 0.3 mM $NaIO_4$ conditions used for peptide exchange the methionine residue on position 5 is partially oxidized, thereby hampering recognition by the T cell receptor (TCR) (Supporting Fig. 5). However, replacement of the oxidizable methionine residue by its isosteric carba-analog[21], norleucine, resulted in successful labeling of CMV positive T cells, whereas application of oxa-isosteres for methionine and cysteine was less fruitful (see Supporting Fig. 6). Isosteric replacement also appeared useful for the detection of T cells specific for the EBV BMLF $I_{(259-267)}$ epitope, in which both a cysteine and methionine residue have been replaced by their carba-analogs (Fig. 5). It is noted that success of isosteric replacement is to some extent donor dependent, as we have observed cases in which isosteric replacement leads to reduced staining efficiency, presumably reflecting a high requirement for complementarity required by the involved T cell receptors (data not shown).

The conditional ligand NLVBMVATV is based on the CMV $pp65_{(495-503)}$ peptide. Although the TCR exposed surface of NLVBMVATV deviates substantially from that of the parental peptide, there is a theoretical possibility that uncleaved peptide remaining after incomplete $NaIO_4$ mediated cleavage would result in staining of CMV $pp65_{(495-503)}$-specific T cells. However, analysis of PBMCs of a CMV positive donor with tetramers prepared from MHC monomers that have not been exposed to $NaIO_4$ do

not display background staining (Supporting Fig. 5). Moreover, the HPLC data in Fig. 3 show that chemocleavage occurs with >98% efficiency.

Chemo-exchange tetramers for T cell enrichment. MHC-based selection of antigen-specific T cells has been proposed as a strategy to boost melanoma-specific T cell responses in individuals with melanoma[22] and to provide defined minor histocompatibility antigen-specific and virus-specific T cells to recipients of allogeneic stem cell transplants and other immunocompromised individuals[23-28]. To provide proof-of-principle for such MHC based T cell selection we used chemo-exchange tetramers in combination with magnetic cell sorting for the isolation of influenza A-specific T cells. As shown in Fig. 6, a single round of MHC-based purification of influenza A $M1_{(58-66)}$-specific T cells from peripheral blood of a healthy donor resulted in a 95 % pure influenza A-specific T cell population.

Discussion

Photomediated MHC exchange technology has shown its merit in various laboratories since we have introduced this technique three years ago[8]. An orthogonal technology that can be used under conditions in which UV-mediated ligand exchange is less feasible involves the use of a chemical trigger to effect peptide exchange reactions. The activating reagent must effect complete and rapid cleavage of the conditional peptide under conditions that do not compromise the functionality of the MHC protein. One example of chemical cleavage of peptide bonds under mild, bioorthogonal conditions is the cleavage of peptides and proteins at azido homoalanine promoted by reducing agents such as phosphines and thiols[29]. However, this cleavage reaction is incomplete under physiological conditions and we therefore focused our chemocleavage strategy on oxidative cleavage of the vicinal diol moiety by the mild oxidant $NaIO_4$.

In an unbiased approach we scanned a vicinal diol containing amino acid residue through various HLA-A2 epitopes with known or predicted affinity and we found that useful chemocleavable peptides have their diol containing residue located on TCR and solvent accessible positions p4 or p5. Accordingly, the replacement of an amino acid residue engaged in TCR interactions, *e.g.* indicated by known crystal structures, seems to be the strategy of choice to adapt the chemocleavage principle to

other MHC alleles. This would omit the necessity of scanning the chemosensitive amino acid residue through an epitope with known affinity.

Our choice for an *anti*-oriented 1,2-diol amino acid building block was guided by the ease of synthesis of Fmoc protected building block **IV** from commercially available (−)-2,3-*O*-isopropylidene-D-erythronolactone **I** in only three steps. However, the crystal structure of HLA-A2.1(Se-Mβ2m)::NLVBMVATV obtained by *in crystallo* exchange indicated a dihedral angle between the conformationally restricted *anti*-hydroxyl groups that seems suboptimal for formation of the intermediate cyclic periodate ester[20]. Nevertheless periodate exposure resulted in >98% cleavage within 2 hours at rt. Periodate triggered MHC exchange may benefit from changing the vicinal diol residue to the *syn* enantiomer, which may favor formation of the cyclic periodate ester intermediate in the MHC bound state and thus increase the rate of the cleavage reaction. Furthermore, a faster cleavage reaction may allow the use of lower periodate concentrations for effective cleavage, which may reduce the occurrence of concomitant oxidation of sulfur containing amino acid residues. We are currently investigating this synthetically more demanding option.

The observed reduced staining efficiency with epitopes containing methionine or cysteine residues due to partial oxidation of sulfur atoms during $NaIO_4$ mediated exchange reactions was circumvented by their isosteric replacement with carba-analogs norleucine and 2-aminobutyric acid, respectively. N-terminal serine or threonine residues in exchange peptides are, however, not compatible with $NaIO_4$ triggered peptide exchange, as their vicinal amino alcohol moiety is prone to oxidative cleavage. However, for T cell staining these particular N-terminal amino acid residues can be replaced by other periodate resistant residues, since p1 is not an MHC class I anchor position and is not involved in decisive interactions with the TCR.

An important application of MHC reagents, use for T cell depletion or enrichment, requires MHC production under sterile conditions. Conditions that can easily be unified by the addition of defined chemicals. Hence, we envisage the use of sterile surfaces, such as tissue culture flasks or tubing, coated with conditional MHC complexes that can be charged with selected epitopes. Peptide exchange may then be effected in a closed sterile environment by the addition of a defined amount of a chemical effector agent. The simplicity of production of different pMHC complexes by MHC exchange may prove valuable for the production of a set of clinical grade MHC reagents for therapeutic purposes. The clinical potential of MHC multimer-based T cell isolation has already been

demonstrated[28] and based on the rapid developments in adoptive T cell therapies[30], we anticipate that MHC multimer-based adoptive T cell therapies will become a prevalent technique.

UV mediated MHC activation often leads to activation of small molecules containing UV sensitive moieties (*e.g.* carbonyl or nitro groups), thereby creating reactive free radical particles and consequently false positives in small molecule screens (B.R., unpublished observation). However, chemically triggered vacation of the MHC binding groove does not have this problem and may find application in high-throughput screening for small molecule MHC binders, while blocking the chemical trigger by addition of a quenching reagent remains an option.

In conclusion, we have shown proof-of-principle for chemically triggered ligand exchange. A chemical trigger that is readily available obviates the need for any special equipment, opening this technique to the broader scientific community. Development of variant chemosensitive ligands that are cleaved under milder conditions will transform this into a platform that can be implemented widely.

Methods

Protein expression and purification. MHC class I refolding reactions were performed as described[9] and class I complexes were purified by gel-filtration HPLC in PBS (pH 7.4). Biotinylation and MHC tetramer formation were performed as described[9].

Fmoc-diol building block and peptide synthesis. The isopropylidene protected diol (*2R,3R*)-4-amino-2,3-dihydroxybutanoic acid (**III**), was obtained from commercially available (−)-2,3-*O*-isopropylidene-D-erythronolactone (**I**) by the method of Kamiya et al.[18]. Subsequent Fmoc protection with fluorenylmethyl chloroformate using standard dioxane-10% aqueous $NaHCO_3$ conditions furnished Fmoc-diol building block **IV** in 72% yield. MS (ESI): $[M+H]^+$ calculated: 398.16, found 398.12. ^{1}H-NMR (400 MHz, d6-DMSO) δ 13.00 (bs, 1H), 7.89 (d, *J* = 7.5 Hz, 2H), 7.71 (d, *J* = 7.5 Hz, 2H), 7.46 and 6.97-6.92 (t and m, *J* = 7.4 Hz, 1H, rotamers), 7.42 (t, *J* = 7.5 Hz, 2H), 7.33 (t, *J* = 7.5 Hz, 2H), 4.60 (d, *J* = 6.8 Hz, 1H), 4.40-4.35 (m, 1H), 4.30 (d, *J* = 6.8 Hz, 2H), 4.22 (t, *J* = 6.8 Hz, 1H), 3.31-3.28 and 2.90-2.97 (m, rotamers, 2H), 1.47 (s, 3H), 1.30 (s, 3H). Naturally occurring peptides and photosensitive and chemosensitive variants were synthesized by standard Fmoc solid phase peptide synthesis and their purity was checked by LC/MS and found to be > 85%.

Conditional peptide exchange and screening for diol peptides. The set of diol containing peptides was subjected to UV mediated peptide exchange with biotinylated conditional HLA-A2.1::GILGFVFJ$_1$L following a protocol that we have reported previously[9]. Briefly, in a 96 well polypropylene plate 50 μL of 0.5 μM biotinylated HLA-A2.1::GILGFVFJ$_1$L (where J$_1$ is UV-cleavable 3-amino-3-(2-nitro)phenyl propionic acid) and 50 μM exchange peptide in PBS was subjected to UV irradiation (366 nm) for 1 h at rt. Following peptide exchange, the plate was divided into two parts of which one part was subjected to treatment with 1 mM $NaIO_4$ for 2 h at 37 °C to enable diol peptide cleavage. A streptavidin based sandwich ELISA was performed as described previously[9] to score for successful peptide exchange and $NaIO_4$ mediated peptide cleavage (and hence MHC degradation). Briefly, wells of 96 well Nunc immunoplate® were coated with streptavidin and following UV-mediated peptide exchange, biotinylated monomers were added to the wells. Bound MHC class I is recognized by horseradish peroxidase conjugated anti-β2m antibodies (DakoCytomation). 2,2'-azino-bis(3-ethylbenzthiazoline-6-sulphonic acid) (ABTS) was added as a substrate for horseradish peroxidase to give a green colored oxidation product, which is monitored at 405 nm, indicative of successful MHC rescue with exchange peptides. Absence of coloring after $NaIO_4$ treatment of MHC monomers indicated efficient peptide cleavage. To produce MHC reagents by chemically induced MHC exchange, we exposed HLA-A2.1::NLVBMVATV (0.5 μM in PBS, pH 7.4) in the presence of 50 μM of the indicated peptide to $NaIO_4$ at the indicated concentration in PBS for 2 h at rt.

Peptide exchange in MHC crystals. Crystallization of HLA-A2.1(Se-Mβ2m)::Se-MILGJ$_2$VFJ$_1$V was performed as described previously (Celie et al., manuscript submitted). The exchange of peptide NLVBMVATV in HLA-A2.1(Se-Mβ2m)::Se-MILGJ$_2$VFJ$_1$V crystals was performed by transferring HLA-A2.1(Se-Mβ2m)::Se-MILGJ$_2$VFJ$_1$V crystals to 4 µl crystallization solution containing 5 mM NLVBMVATV peptide in the sub-wells of a 96-well Greiner Crystal Quick Low-Profile crystallization plate. Crystals in solution were exposed 3 to 6 times to UV light (366 nm UV lamp, 2x15W blacklight blue tubes, LxWxH 505x140x117 mm, Uvitec, UK, 10 cm distance from sample) for 10 minutes at 4 °C, with 2 minutes intervals. After UV irradiation, the plate was sealed with Hampton ClearSeal and

left for 4 hrs at 20 °C, allowing cleaved peptide fragments to dissociate and to be exchanged for the NLVBMVATV peptide. Crystals were vitrified and stored at -80 °C.

Data collection, processing and structure refinement. Diffraction data for HLA-A2.1(Se-Mβ2m):: NLVBMVATV were collected at a temperature of 100 K using synchrotron radiation on beamline PXI X06SA, SLS, Villigen, Switzerland. Data were collected on a single crystal at a wavelength of 0.979 Å. The wavelength was optimized for measuring the anomalous scattering of the selenium atoms. All diffraction data were integrated with MOSFLM[31] and scaled in SCALA[32]. Crystals belong to the monoclinic space group $P2_1$, with a β angle close to 90^o degrees and are pseudo-merohedrally twinned. Molecular replacement using an HLA-2.1 structure with the ligand removed was performed with AMORE through the CCP4i interface[33]. The positioned model was refined in REFMAC[34]. Manual inspection, rebuilding and the placement of the peptide was done with Coot[35]. Restrain libraries for non-standard amino-acids were created in the CCP4i sketcher and LIBCHECK. Final refinement was performed in PHENIX[36]. The exchange efficiency was validated by measuring the anomalous density of selenium atoms in the β2m protein and residual anomalous density at the positions previously occupied by the Se atoms in position p1 of the UV conditional ligand. The anomalous difference map clearly shows the presence of selenium atoms for Se-M residues 0 and 99 in Se-Mβ2m, but no residual density for Se-M of the photosensitive conditional peptide (Supporting Fig. 2). The structure was validated in Coot and WHATCHECK[37] and is submitted to the Protein Databank (XXX.pdb). Within the final model, 92.7% of the amino acids are in preferred regions of the Ramachandran plot, 5.7% in allowed regions and 1.6% are considered outliers.

Exchange Kinetics. Chemically induced exchange kinetics were monitored by gel-filtration HPLC on a Biosep SEC S-3000 column (Phenomenex) in line with a fluorescence detector by performing MHC exchange of HLA-A2.1 refolded with fluorescently labeled NLVBMVAC(Fl)V in the presence of 50 μM cytomegalovirus $pp65_{(495-503)}$ epitope NLVPMVATV. Labeling of peptides with tetramethylrhodamine-5-maleimide (Tebu-bio) was performed as described[10]. Exchange was started by the addition of 0.3 mM $NaIO_4$ in PBS at rt. Data were analyzed by using GraphPad Prism software (GraphPad).

Cells and flow cytometry. For analysis of MHC tetramer binding and T cell responses in human samples, peripheral blood mononuclear cells of healthy volunteers were obtained by Ficolll gradient separation. Cells were stained with the indicated MHC tetramers for 4 min at 37 °C. Subsequently, cells were incubated with anti-CD8 antibody (BD Biosciences) for 10 to 15 min at 15 to 25 °C. Data acquisition and analysis was carried out on a FACSCalibur (Becton Dickinson) using FlowJo software.

T cell enrichment. For T cell enrichment using magnetic cell sorting with MACS™ beads, $2x10^7$ PBMCs of a healthy donor were stained with 50 μL of a sample of 12.5 μg/mL phycoerythrin-conjugated diol exchange tetramers of HLA-A2.1::influenza A $M1_{(58-66)}$ epitope. Staining was performed at rt. for 30 min in Iscove's medium supplemented with 10 % human serum. Subsequently, cells were washed with medium and 40 μL MACS™ anti- PE beads was added. After a 15 min incubation at 4 °C, cells were washed and enriched on a MACS™ column following the manufacturer's protocol. After elution of enriched cells from the column, cells were restained with PE conjugated diol exchange tetramers of HLA-A2.1:: influenza A $M1_{(58-66)}$ and FITC-conjugated anti-CD8 antibody and analyzed by flow cytometry.

Acknowledgments

We thank Henk Hilkmann for peptide synthesis. We are grateful to the PXI beamline scientists at SLS (Villigen, Switserland) for assistance during data collection experiments.

Supporting Information Available

Crystallographic data collection and refinement statistics, crystal structures, ELISA data, LC-MS analysis and kinetic analysis of conditional peptide cleavage and FACS data. This material is available free of charge via the Internet at http://pubs.acs.org.

Competing interests statement

M.T., H.O and T.N.M.S. declare competing financial interests.

Statement:

The MHC exchange technology described in this manuscript is the subject of a patent. Based on Netherlands Cancer Institute policy on management of intellectual property, M.T., H.O and T.N.M.S. would be entitled to a portion of received royalty income in case of future licensing.

References

1. Fremont, D. H.; Matsumura, M.; Stura, E. A.; Peterson, P. A.; Wilson, I. A. *Science* **1992,** *257*, 919-927.

2. Silver, M. L.; Guo, H. C.; Strominger, J. L.; Wiley, D. C. *Nature* **1992,** *360*, 367-369.

3. Bouvier, M.; Wiley, D. C. *Science* **1994,** *265*, 398-402.

4. Schumacher, T. N.; De Bruijn, M. L.; Vernie, L. N.; Kast, W. M.; Melief, C. J.; Neefjes, J. J.; Ploegh, H. L. *Nature* **1991,** *350*, 703-706.

5. Ljunggren, H. G.; Stam, N. J.; Ohlen, C.; Neefjes, J. J.; Hoglund, P.; Heemels, M. T.; Bastin, J.; Schumacher, T. N. M.; Townsend, A.; Kärre, K.; Ploegh, H. L. *Nature* **1990,** *346*, 476-480.

6. Schumacher, T. N.; Heemels, M. T.; Neefjes, J. J.; Kast, W. M.; Melief, C. J.; Ploegh, H. L. *Cell* **1990,** *62*, 563-567.

7. Garboczi, D. N.; Hung, D. T.; Wiley, D. C. *Proc. Natl. Acad. Sci. U S A* **1992,** *89*, 3429-3433.

8. Toebes, M.; Coccoris, M.; Bins, A.; Rodenko, B.; Gomez, R.; Nieuwkoop, N. J.; van de Kasteele, W.; Rimmelzwaan, G. F.; Haanen, J. B.; Ovaa, H.; Schumacher, T. N. *Nat. Med.* **2006,** *12*, 246-251.

9. Rodenko, B.; Toebes, M.; Hadrup, S. R.; van Esch, W. J.; Molenaar, A. M.; Schumacher, T. N.; Ovaa, H. *Nat. Protoc.* **2006,** *1*, 1120-1132.

10. Bakker, A. H.; Hoppes, R.; Linnemann, C.; Toebes, M.; Rodenko, B.; Berkers, C. R.; Hadrup, S. R.; van Esch, W. J. E.; Heemskerk, M. H. M.; Ovaa, H.; Schumacher, T. N. M. *Proc. Natl. Acad. Sci. U S A* **2008,** *105*, 3825-3830.

11. Grotenbreg, G. M.; Roan, N. R.; Guillen, E.; Meijers, R.; Wang, J. H.; Bell, G. W.; Starnbach, M. N.; Ploegh, H. L. *Proc. Natl. Acad. Sci. USA* **2008,** *105*, 3831-3836.

12. Gredmark-Russ, S.; Cheung, E. J.; Isaacson, M. K.; Ploegh, H. L.; Grotenbreg, G. M. *J. Virol.* **2008,** *82*, 12205-12212.

13. Frickel, E. M.; Sahoo, N.; Hopp, J.; Gubbels, M. J.; Craver, M. P.; Knoll, L. J.; Ploegh, H. L.; Grotenbreg, G. M. *J. Infect. Dis.* **2008,** *198*, 1625-1633.

14. Grotenbreg, G. M.; Nicholson, M. J.; Fowler, K. D.; Wilbuer, K.; Octavio, L.; Yang, M.; Chakraborty, A. K.; Ploegh, H. L.; Wucherpfennig, K. W. *J Biol Chem* **2007,** *282*, 21425-21436.

15. Soen, Y.; Chen, D. S.; Kraft, D. L.; Davis, M. M.; Brown, P. O. *PLoS. Biol* **2003,** *1*, E65.

16. Chen, D.; Soen, Y.; Stuge, T.; Lee, P.; Weber, J.; Brown, P.; Davis, M. *PLoS Medicine* **2005,** *2*.

17. Stone, J.; Demkowicz, W. E., Jr.; Stern, L. *Proc. Natl. Acad. Sci. USA* **2005,** *102*, 3744-3749.

18. Kamiya, T.; Saito, Y.; Seki, H.; Hashimot, M. *Tetrahedron* **1972,** *28*, 899-906.

19. Madden, D. R.; Garboczi, D. N.; Wiley, D. C. *Cell* **1993,** *75*, 693-708.

20. Buist, G. J.; Bunton, C. A.; Hipperson, W. C. P. *J. Chem. Soc. B* **1971,** 2128-2142.

21. Moroder, L. *J. Pept. Sci.* **2005,** *11*, 187-214.

22. Yee, C.; Savage, P. A.; Lee, P. P.; Davis, M. M.; Greenberg, P. D. *J. Immunol.* **1999,** *162*, 2227-2234.

23. Falkenburg, J. H.; van de Corp; Marijt, E. W.; Willemze, R. *Exp. Hematol.* **2003,** *31*, 743-751.

24. Moss, P.; Rickinson, A. *Nat. Rev. Immunol.* **2005,** *5*, 9-20.

25. Peggs, K. S.; Verfuerth, S.; Pizzey, A.; Khan, N.; Guiver, M.; Moss, P. A.; Mackinnon, S. *Lancet* **2003,** *362*, 1375-1377.

26. Rooney, C. M.; Smith, C. A.; Ng, C. Y.; Loftin, S.; Li, C.; Krance, R. A.; Brenner, M. K.; Heslop, H. E. *Lancet* **1995,** *345*, 9-13.

27. Walter, E. A.; Greenberg, P. D.; Gilbert, M. J.; Finch, R. J.; Watanabe, K. S.; Thomas, E. D.; Riddell, S. R. *N. Engl. J. Med.* **1995,** *333*, 1038-1044.

28. Cobbold, M.; Khan, N.; Pourgheysari, B.; Tauro, S.; McDonald, D.; Osman, H.; Assenmacher, M.; Billingham, L.; Steward, C.; Crawley, C.; Olavarria, E.; Goldman, J.; Chakraverty, R.; Mahendra, P.; Craddock, C.; Moss, P. A. *J. Exp. Med.* **2005,** *202*, 379-386.

29. Back, J. W.; David, O.; Kramer, G.; Masson, G.; Kasper, P. T.; de Koning, L. J.; de Jong, L.; van Maarseveen, J. H.; de Koster, C. G. *Angew. Chem. Int. Ed. Engl.* **2005,** *44*, 7946-7950.

30. Rosenberg, S. A.; Restifo, N. P.; Yang, J. C.; Morgan, R. A.; Dudley, M. E. *Nat. Rev. Cancer* **2008,** *8*, 299-308.

31. Leslie, A. G. W. *Joint CCP4 + ESF-EAMCB Newsletter on Protein Crystallography* **1992,** *26*.

32. Evans, P. R. *Joint CCP4 and ESF-EACBM Newsletter* **1997,** *33*, 22-24.

33. CCP4 (Collaborative Computational Project, No. 4. *Acta Crystallogr. D Biol. Crystallogr.* **1994,** *50*, 760-763.

34. Murshudov, G. N.; Vagin, A. A.; Dodson, E. J. *Acta Crystallogr. D Biol. Crystallogr.* **1997,** *53*, 240-255.

35. Emsley, P.; Cowtan, K. *Acta Crystallogr. D Biol. Crystallogr.* **2004,** *60*, 2126-2132.

36. Adams, P. D.; Grosse-Kunstleve, R. W.; Hung, L. W.; Ioerger, T. R.; McCoy, A. J.; Moriarty, N. W.; Read, R. J.; Sacchettini, J. C.; Sauter, N. K.; Terwilliger, T. C. *Acta Crystallogr. D Biol. Crystallogr.* **2002,** *58*, 1948-1954.

37. Vriend, G. *J. Mol. Graph.* **1990,** *8*, 52-6, 29.

38. Bosques, C. J.; Imperiali, B. *J. Am. Chem. Soc.* **2003,** *125*, 7530-7531.

39. Rammensee, H.; Bachmann, J.; Emmerich, N. P.; Bachor, O. A.; Stevanovic, S. *Immunogenetics* **1999,** *50*, 213-219.

Figure and Scheme Legends

Figure 1. The principle of conditional MHC class I. (a) Conditional MHC class I is treated with a trigger, which cleaves the conditional peptide ligand to afford two fragments that no longer meet minimal affinity requirements and dissociate from the peptide binding groove. The resulting ligand-receptive MHC class I has a short half-life at 37 ºC if not stabilized by the binding of a 'rescue' ligand. (b) Photocleavage of a 2-nitrophenyl containing conditional peptide ligand triggered by 365 nm UV light[38]. (c) Chemo-cleavage of a vicinal diol containing conditional peptide ligand triggered by the addition of $NaIO_4$.

Figure 2. Crystal structure of HLA-A2.1(Se-Mβ2m)::NLVBMVATV. (a) Overall structure of HLA-A2.1(Se-Mβ2m)::NLVBMVATV. HLA-A2.1 is shown as a cartoon with the α1 domain in cyan, the α2 domain in slate, the α3 domain in marine and Se-Mβ2m in green. Peptide NLVBMVATV is represented as sticks, with carbons in yellow, nitrogen in blue, oxygen in red and sulfur in orange. (b) Peptide is shown in the same orientation as in (a), together with the final 2mFO-DFc electron density map (blue) displayed at a contour level of 1.0 sigma and a radius of 1.8 Å around the peptide. (c) Structure of HLA-A2.1::NLVPMVATV, (Celie et al., submitted for publication) is superimposed on the HLA A2.1(Se-Mβ2m)::NLVBMVATV structure to illustrate the conformational similarities. Peptide NLVBMVATV is represented as in (b) and peptide NLVPMVATV is shown with carbons in cyan.

Figure 3. Peptide exchange efficiency and kinetics as monitored by gel-filtration HPLC analysis using UV absorbance (230 nm, left) and fluorescence (550ex/567em, right) detection. (a) Chemo-exchange of 0.5 µM HLA-A2.1::NLVBMVAC(Fl)V by treatment with 0.3 mM $NaIO_4$ in the presence of 50 µM NLVPMVATV at rt. (b) Photo-exchange of 0.5 µM HLA-A2.1::KILGC(Fl)VFJ_1V by exposure to UV light (365 nm) in the presence of 50 µM NLVPMVATV at rt. (c) Treatment of HLA-A2.1::KILGC(Fl)VFJ_1V with $NaIO_4$ in the presence of NLVPMVATV.

Figure 4. Detection of antigen-specific T cells using chemo-exchange MHC multimers. Analysis of MHC tetramer staining of peripheral blood mononuclear cells of a healthy donor with the indicated MHC tetramers: HLA-A2.1::influenza $M1_{(58-66)}$ obtained via UV exchange (top left), HLA-A2.1::influenza

$M1_{(58-66)}$ obtained via chemo-exchange (bottom). No staining is seen for conditional HLA-A2.1 loaded with diol peptide NLVBMVATV (top right). Numbers indicate the percentage of MHC tetramer^{+} cells of $CD8^{+}$ cells.

Figure 5. Staining of peripheral blood mononuclear cells of healthy donors with HLA-A2.1 exchange tetramers obtained by either UV or $NaIO_4$ mediated exchange as indicated. CMV: CMV $pp65_{(495-503)}$ epitope NLVPMVATV; CMV-Met5Nle: CMV $pp65_{(495-503)}$ epitope in which methionine is replaced with norleucine (Nle); EBV: EBV-BMLF $I_{(259-267)}$ epitope; EBV-Cys3Abu-Met8Nle: EBV-BMLF $I_{(259-267)}$ epitope, in which cysteine is replaced with L-2-aminobutyric acid and methionine is replaced with norleucine; Numbers indicate the percentage of MHC tetramer^{+} cells of $CD8^{+}$ cells.

Figure 6. T cell enrichment using chemo-exchange tetramers for magnetic cell sorting. For T cell enrichment using magnetic cell sorting, peripheral blood mononuclear cells of a healthy donor were stained with PE-conjugated tetramers of HLA-A2.1::influenza A $M1_{(58-66)}$ obtained via chemo-exchange methodology. Attachment of the stained T cells to anti-PE MACS™ beads followed by purification using a magnetic column resulted in a T cell sample enriched from 0.3 % before treatment (left panel) to 95% pure influenza A $M1_{(58-66)}$-specific T cells (right panel).

Scheme 1. Synthesis of vicinal diol containing amino acid building block **IV** for use in Fmoc based automated peptide synthesis. a) potassium phtalimide, DMF, reflux. b) hydrazine, EtOH, reflux. c) FmocCl, $NaHCO_3$-H_2O, dioxane.

Tables

Table 1. Chemocleavable amino acid scan through various HLA-A2.1 epitopes and assessment of MHC binding and chemocleavage by ELISA.[a]

No.	Sequence	No $NaIO_4$ treatment (% of control ± SEM)	$NaIO_4$ treatment (% of control ± SEM)	No.	Sequence	No $NaIO_4$ treatment (% of control ± SEM)	$NaIO_4$ treatment (% of control ± SEM)
1	NLVPMVATV[b]	100 ± 0.0	81 ± 3.1	25	YLLP**B**GPRL	84 ± 3.6	12 ± 0.2
2	NL**B**PMVATV	6 ± 1.4	2 ± 1.3	26	YLLPR**B**PRL	58 ± 4.7	8 ± 0.3
3	NLV**B**MVATV	91 ± 8.0	4 ± 0.9	27	YLLPRR**B**RL	19 ± 1.9	3 ± 0.7
4	NLVP**B**VATV	76 ± 5.6	12 ± 1.6	28	FLPSDFFPSV[f]	63 ± 3.5	50 ± 1.3
5	NLVPM**B**ATV	49 ± 1.9	11± 1.3	29	FL**B**DFFPSV	59 ± 3.6	42 ± 3.4
6	NLVPMV**B**TV	2 ± 0.9	2 ± 1.0	30	FLP**B**FFPSV	61 ± 3.6	6 ± 0.1
7	NLVPMVA**B**V	2 ± 0.9	1 ± 0.9	31	FLPS**B**FPSV	66 ± 3.3	26 ± 0.4
8	KILGFVFTV[c]	32 ± 7.6	39 ± 6.1	32	FLPSD**B**PSV	81 ± 2.9	49 ± 0.5
9	KI**B**GFVFTV	7 ± 1.3	8 ± 0.4	33	FLPSDF**B**SV	81 ± 1.7	58 ± 2.0
10	KIL**B**FVFTV	50 ± 3.0	5 ± 0.0	34	ILAETVVAKV[g]	48 ± 3.0	40 ± 2.3
11	KILG**B**VFTV	43 ± 2.6	7 ± 0.3	35	IL**B**TVVAKV	6 ± 0.8	6 ± 0.2
12	KILGF**B**FTV	55 ± 5.0	3 ± 0.1	36	ILAETVV**B**V	48 ± 3.9	7 ± 1.0
13	KILGFV**B**TV	48 ± 4.4	30 ± 1.2	37	ILA**B**VVAKV	55 ± 3.0	3 ± 0.4
14	KILGFVF**B**V	31 ± 3.1	20 ± 0.0	38	IL**B**TVAKV	41 ± 3.6	27 ± 0.6
15	ILAETVAKV[d]	74 ± 9.9	61 ± 3.7	39	ILA**B**VAKV	38 ± 2.9	12 ± 0.3
16	IL**B**ETVAKV	10 ± 1.5	5 ± 0.3	40	ILAE**B**AKV	68 ± 7.0	46 ± 1.7
17	ILA**B**TVAKV	71 ± 14.0	2 ± 0.9	41	ILAET**B**KV	16 ± 2.3	7 ± 0.8

18	ILAE**B**VAKV	66 ± 11.9	5 ± 0.2	42	SLYNTVATL[h]	52 ± 6.1	39 ± 2.2
19	ILAET**B**AKV	53 ± 6.2	12 ± 0.3	43	SL**B**NTVATL	1 ± 0.9	-1 ± 0.1
20	ILAETV**B**KV	52 ± 2.6	28 ± 0.6	44	SLY**B**TVATL	62 ± 8.3	2 ± 0.0
21	ILAETVA**B**V	45 ± 3.9	6 ± 0.5	45	SLYN**B**VATL	53 ± 6.5	2 ± 0.3
22	YLLPRRGPRL[e]	66 ± 5.2	51 ± 3.0	46	SLYNT**B**ATL	46 ± 6.6	28 ± 2.1
23	YL**B**RRGPRL	7 ± 0.2	1 ± 0.5	47	SLYNTV**B**TL	0 ± 0.0	0 ± 0.0
24	YLL**B**RGPRL	80 ± 4.2	8 ± 0.8	48	SLYNTVA**B**L	2 ± 0.3	0 ± 0.3

a) Following UV mediated ligand exchange with 0.25 μM HLA-A2.1::GILGFVFJ_1L, 50 μM diol peptide and 1 hr irradiation at 365 nm an ELISA[9] was performed with 5 nM exchanged HLA-A2.1 untreated or after treatment with 1 mM $NaIO_4$ for 2 h at 37 ºC. Absorbance at 405 nm was normalized to exchanged HLA-A2.1::peptide **1** without $NaIO_4$ treatment. b) cytomegalovirus $pp65_{(495-503)}$ c) influenza A Matrix $1_{(58-66)}$ in which G1 is replaced with K for solubility reasons and in which anchor residue L9 is replaced with V for increased HLA affinity; d) SIFPEITHI score 34, predicted optimal binder using the SYFPEITHI dataset[39] e) hepatitis C virus core $protein_{(35-44)}$ f) hepatitis B virus $nucleocapsid_{(18-27)}$, g) SIFPEITHI score 34, predicted optimal binder using SYFPEITHI dataset, h) HIV-1 (BRU) gag $p17_{(76-84)}$.

Figure 1

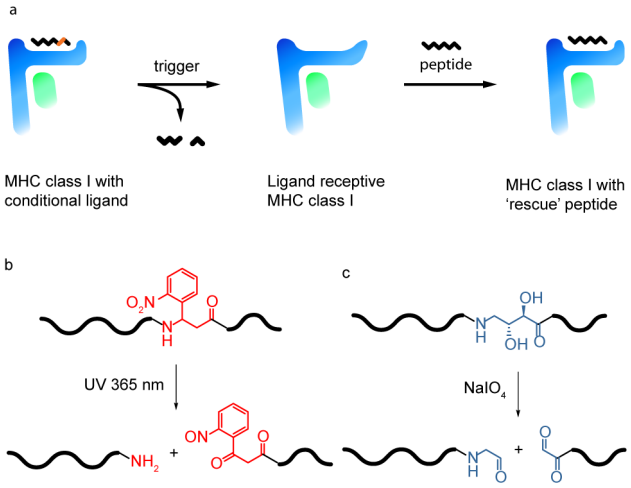
a
trigger
peptide
MHC class I with conditional ligand
Ligand receptive MHC class I
MHC class I with 'rescue' peptide
b
UV 365 nm
c
NaIO4

Figure 2

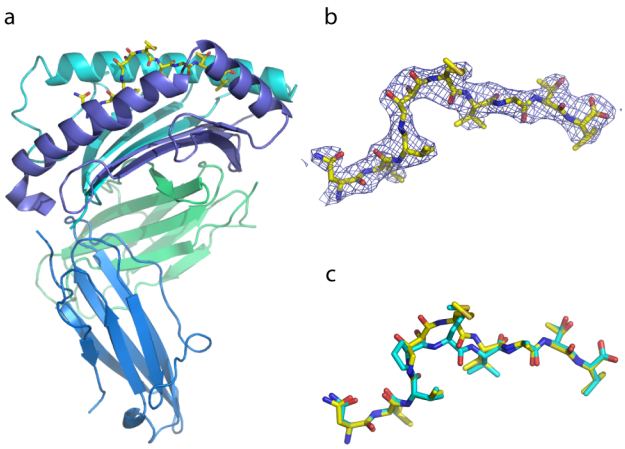

Figure 3

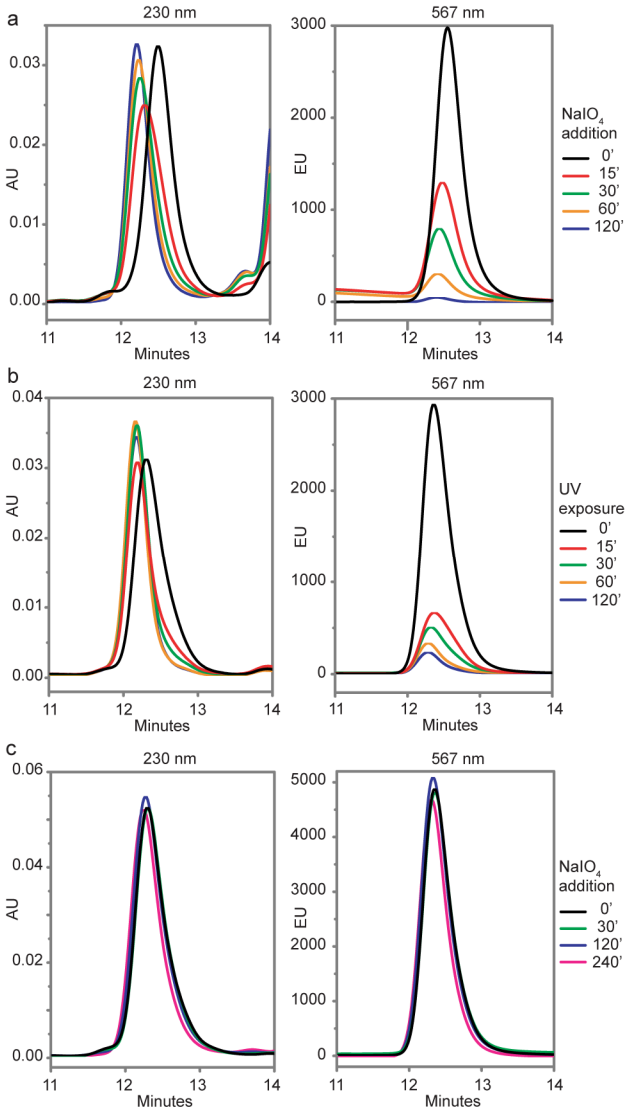
a
230 nm
567 nm
AU
EU
Minutes
NaIO4 addition
0'
15'
30'
60'
120'
b
230 nm
567 nm
AU
EU
Minutes
UV exposure
0'
15'
30'
60'
120'
c
230 nm
567 nm
AU
EU
Minutes
NaIO4 addition
0'
30'
120'
240'

Figure 4

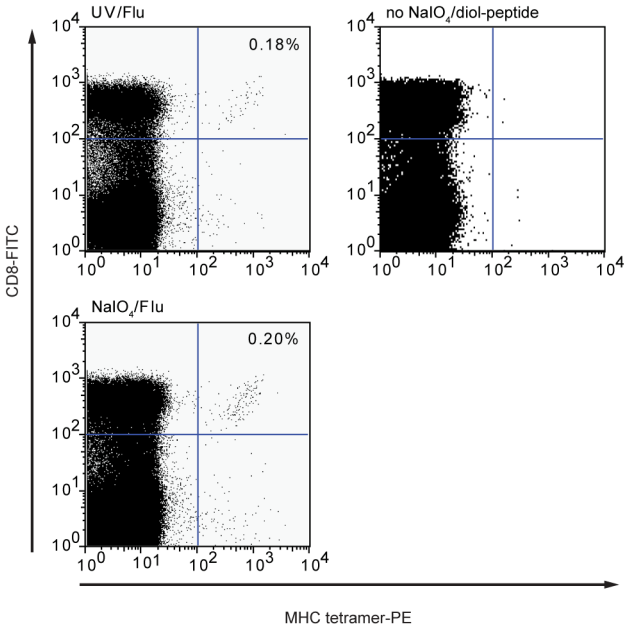
UV/Flu
0.18%
no NaIO4/diol-peptide
NaIO4/Flu
0.20%
CD8-FITC
MHC tetramer-PE

Figure 5

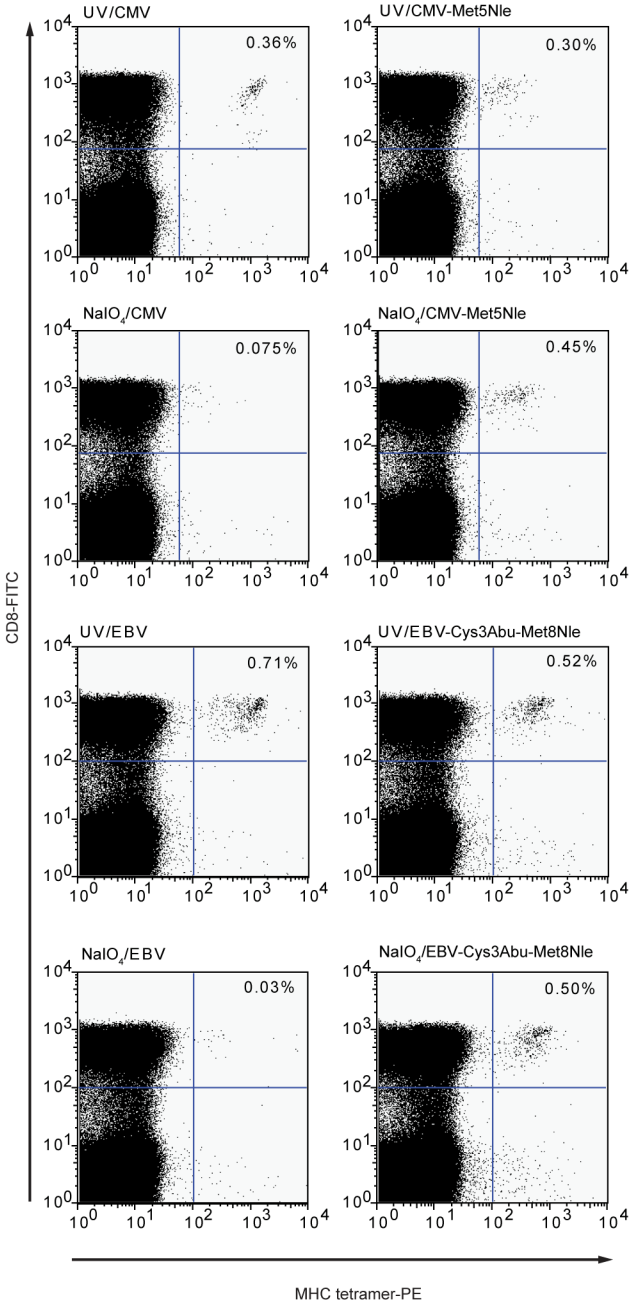
UV/CMV
0.36%
UV/CMV-Met5Nle
0.30%
NaIO4/CMV
0.075%
NaIO4/CMV-Met5Nle
0.45%
UV/EBV
0.71%
UV/EBV-Cys3Abu-Met8Nle
0.52%
NaIO4/EBV
0.03%
NaIO4/EBV-Cys3Abu-Met8Nle
0.50%
CD8-FITC
MHC tetramer-PE

Figure 6

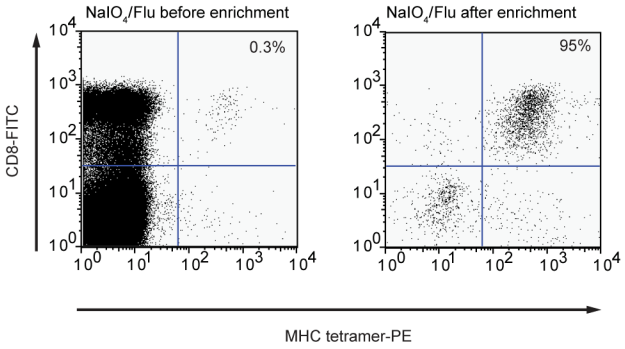
NaIO4/Flu before enrichment
0.3%
NaIO4/Flu after enrichment
95%
CD8-FITC
MHC tetramer-PE

Scheme 1

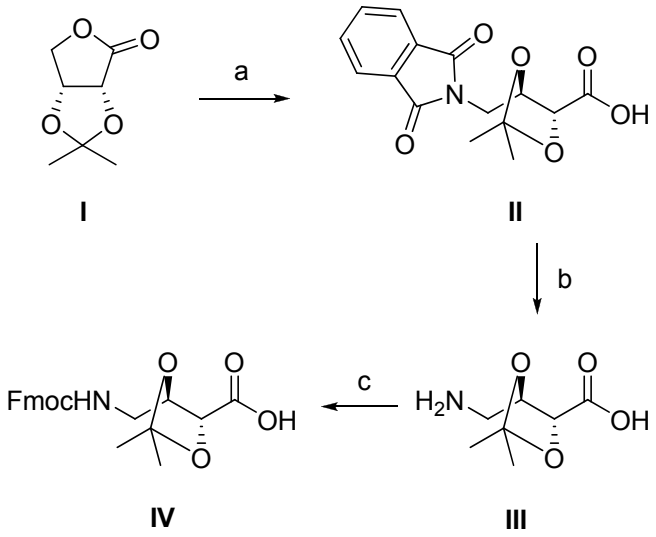

TOC graphic

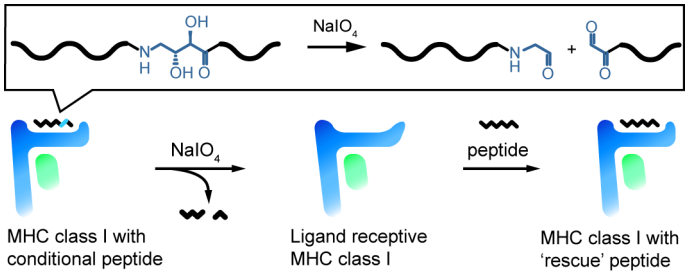
OH
N
H
OH O
NaIO4
N
H
O
+
O
O
NaIO4
peptide
MHC class I with
conditional peptide
Ligand receptive
MHC class I
MHC class I with
'rescue' peptide